ADVANCED PHYSICS RESEARCH Open Access
www.advphysicsres.com

Nanoprobe Based Information Processing: Nanoprobe-Electronics

*Bao Yi, Long You, and Jeongmin Hong**

With computational architectures becoming data-centric and with the rise of in-memory computing, the role of memory will be ever more crucial. In turn, storing massive amount of data demands for ultra-low power and non-volatile types necessitating new memory technologies. Here, a controllable nanoelectromechanical (NEM) spin memory is proposed for compact nonvolatile memory arrays. It combines the advantages of both nanomechanical and spin-transfer torque (STT) magnetic memory devices to overcome fundamental scalability roadblocks of non-hybrid alternatives. The hybrid system paves the way to a new memory technology in the regime of sub-10-nm lateral size with a sub-1-MA cm^{-2} switching energy.

1. Introduction

Spintronic devices are one of the candidates for their nonvolatility with sufficiently high endurance that satisfies the ever-growing requirement for nonvolatile and recyclable working memory in state-of-the-art information and communication technology (ICT) systems.[1] Another nonvolatile memory technology that could be scaled to an even higher areal densities utilizes nanoelectromechanical systems (NEMS).[2] If combined, these two technologies might provide the memory capabilities that are unmatched by any other alternative.

Flash memory market is the fastest growing memory sector because of the continuously increasing demand for portable electronics.[3] So far, memory cell size reduction increases storage capacity and the density of the device stacks while lowering cost per bit. However, fundamental scaling limitations for the flash memory cell operating voltages and the physical thickness of the tunneling dielectric layer pose a significant challenge for continued scaling in the sub-10-nm regime.[4] Therefore, alternative systems and structures have been proposed to overcome the scaling bottleneck of the conventional memory cell.[2] The pursuits of a variety of memory technologies have been attempted to succeed the current flash memory technology because they allow for the most compact durable data storage and can be fabricated using a relatively simple process that is more suitable for 3D integration, arguably the emerging trend in next-generation information processing industries.[5,6]

Programmable resistance devices such as phase-change memory (PC-RAM) and resistive RAM (ReRAM) have been explored for cross-contact memory applications, but generally require a selector device within each memory cell to reduce unwanted leakage current through unselected cells during a read operation; otherwise, the size of the array will be severely limited, resulting in poor memory-array area efficiency. The selector devices require additional process steps and can significantly reduce the cell current, resulting in a slower read operation.

Nonvolatile memory is promising due to its stability, scalability, and longer retention.[7] There are two main potential contenders for next-generation nonvolatile memory, magnetoresistive (MR) memory, and nanomechanical memory, respectively.[8,9] Each contender has its pros and cons. MR devices are known to have superior non-volatility and recyclability, while nanomechanical devices offer superior scalability. Here, we present a study on a nanoprobe-based memory device that leverages the advantages of both spintronics and NEMS technologies.

2. Results and Discussion

The NEM switching under study was controlled by scanning probe microscopy (SPM).[9] The tip and the substrate in this experiment were fabricated using a special nanofabrication process as reported in our previous publications.[10] Each side of the structure contained a magnet with an insulation layer and the structure shows a strong perpendicular magnetic anisotropy (PMA).[11,12] We investigated a new device that exploits the advantages of both the NEMS and spintronic technologies. Particularly, we demonstrated that nanomagnets placed on the NEM elements

J. Hong
School of Sciences
Hubei University of Technology
Wuhan 430068, P. R. China
E-mail: jehong@hbut.edu.cn

B. Yi, L. You
School of Optical and Electronic Information
Huazhong University of Science and Technology
Wuhan 430074, P. R. China

J. Hong
EECS
UC Berkeley
Berkeley, CA 9420, USA

The ORCID identification number(s) for the author(s) of this article can be found under https://doi.org/10.1002/apxr.202300076

DOI: 10.1002/apxr.202300076

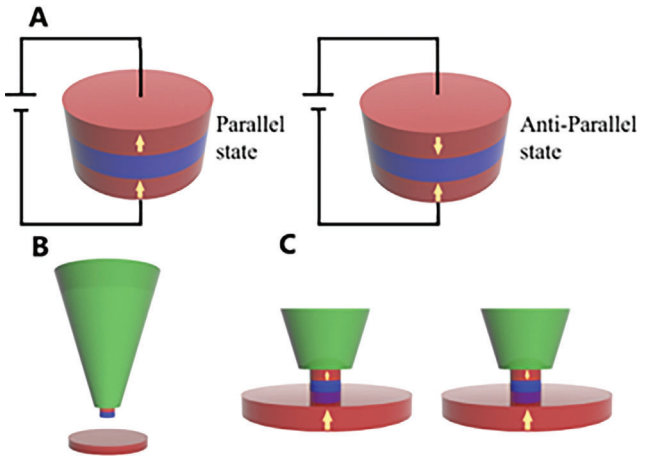

Figure 1. The overall schematics of the probe–based device structures. There are two sides of the structures: one is probe and the other is magnetic substrates. Nanoprobe based spin transfer torque magnetic tunnel junction structures (STT-MTJs). A) MTJ devices with parallel state on the left. MTJ devices with anti-parallel state on the right. Spin-polarized currents change the magnetization direction on media side. B) A Nanoprobe-base magnetic tunnel junction. C) All-in-one probe based magnetic device with magnetic tunnel junction stacks on top of the probe.

could be used as highly scalable non-volatile, and robustly controlled memory. The STT switching experiments conducted on extremely high-anisotropy $L1_{(0)}$ phase media showed a remarkably energy-efficient switching capability.

Figure 1A shows the schematic concept of the device and there are two sides of the structures: one is a probe and the other is magnetic substrates. Nano-probe based spin transfer torque magnetic tunnel junction structures (STT-MTJs) show two states: parallel state ("on" state) and anti-parallel state ("off" state). Spin-polarized currents change the magnetization direction on media side. A full Nano-probe-based magnetic tunnel junction shows all-in-one probe based magnetic device with magnetic tunnel junction stacks on top of the probe.

For a variety of practical memory operations, we tested two alternative probe-media configurations as shown in Figure 1B. First, it is "half magnet probe", with one magnet on each side, the probe and media, respectively. Here, we test half probe with high stability, with an $L1_{(0)}$ ordered magnet on the media side. The second is "all-in-one probe", with both magnets separated by an insulation layer, all deposited on the probe-side as shown in Figure 1C. All the configurations offer alternative ways to test the hybrid approach. For low energy switching, the all-in-one probe shows continuous scaling down to the sub-5-nm size range. We calculated the size of the structure by the resistance and assumed the maximum resistance will sub-5-nm range. Half junctions with high density spins, on the order of 10^5 spins, ensure switching relatively large high-stability media structures.

Programmable point contact measurement could perform high sensitivity transport measurements. While the current was applied, the probe was approaching the sample surface very closely as the "point contact" state by the control of piezo element mounted in SPM. The current between the tip and substrate controls the size of the contract point. The mechanism is equivalent to the conductive AFM. The resistance will be measured to define the size of the contract regions. For the fabrication of the functional probe, the standard stacks of W/ CoCr (10 nm)/ Ta (5 nm)/ CoFeB (1 nm)/ MgO (0.9 nm) on tip side were deposited as shown in **Figure 2**A. State-of-the-art He+ based focused ion beam (FIB) trimming was used to develop a nanoscale magnetic structure on top of the tip as shown in Figure 2A. A perpendicular CoFeB structure was trimmed by focused ion beam etching performed by an Orion NanoFab system with He and Ne ion beams. From the pristine W probe, several thin film stacks were deposited on the top of the probes and FIB was milled to isolate the region.

From the substrate side, Ta/ FePt/ MgO thin film stacks were fabricated, as also shown in Figure 2B. The media with a high perpendicular magnetic anisotropy, on the order of 106 erg cc^{-1}, was fabricated through a standard lithographic process. Final fabricated probe is shown in Figure 2B. The fabricated media structure was carefully tested via ultrahigh sensitive AFM in conjunction with MFM as shown in Figure 2C. The structure showed a single domain state with a coercivity field of 50 Oe.

Figure 2D shows the probe writer. The left image illustrated the normal states which have two resistance states: one is from "probe" side and the other is "media" side. While sweeping

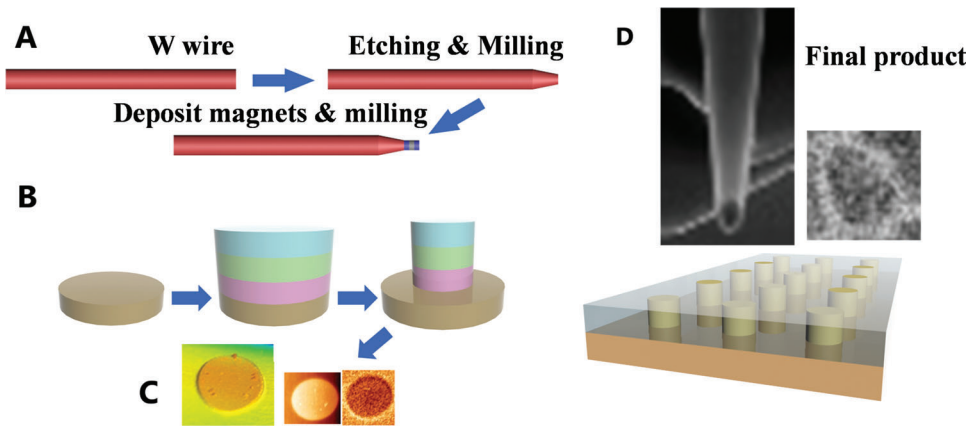

Figure 2. Probe fabrication of memory writer. A) A descriptive schematic of the device: a concept of writing the other magnet from the probe manipulated by NEM switching. B) Fabrication process and final product of the media. C) AFM (left) /MFM (right) images of the final product. D) An illustrative schematics of probe spin memory operation. The measured size of the media is 50 nm.

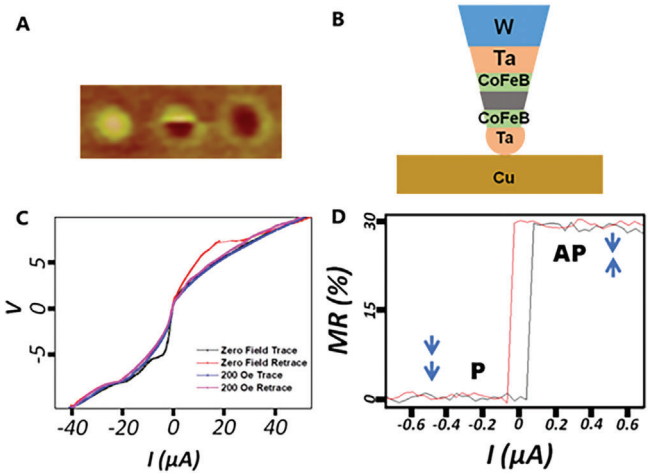

Figure 3. All-in-one nanoprobe based computing device structure. A) Current-induced magnetization change in media. Magnetic SPM micrograph shows the corresponding images of magnetization changes by varying the current states. The size of the structure is ≈10 nm. B) A schematic of the final structure. From the top Ta, CoFeB, MgO, CoFeB, and Ta are deposited. The bottom Ta layer can be approaching to the media, a yellow layer. C) Magnetic field dependence of *I–V* characteristics of the device. IV characteristics of both probe and media stack with an applied magnetic field. D) While the probe and media establish the nanosized contact "nanopoint-contact", current Versus resistance characteristics determined very small switching energy and %MR.

current, the point contacts make a single resistance state. The images indicate that the full system configurations pass spin polarized current to change the magnetization direction. The SEM shows an image of the media structure.

As shown in **Figure 3**A, we tested a current dependent magnetization change to randomly switch the media. SPM results on the bottom show the change of magnetization by sweeping the current. Above the switching current, the images are clearly switched as shown in Figure 3A. From the study, the magnetization of the media can be easily controllable with the probe head to switch perpendicularly magnetized both CoFeB and FePt-based media stacks.

The micrographs on the top of Figure 3A indicate programmable current changes during the magnetic imaging. The imaging corresponds to the change of the current from the probe. Under the switching energy, the image (magnetization) was flipped to red or yellow color. The switching phenomena mean that magnetization is changed with respect to the change of the switching energy variations.

Figure 3B,C show the schematic of the structure and the resulting I–V characteristics using magnetic field dependence, respectively. Magneto-transport measurement using point contact shows the magnetization switching. Under the presence of no magnetic field, parallel and anti-parallel switching was clearly observed. Above the saturation magnetic field, the dependence decays. The top left image shows the actual media structure which consists of Ta/ CoFeB/ MgO thin film stacks. The switching current was measured to be on the order of 10 μA with the current sweep range of 50 μA was chosen.

A more suitable model would consider a material in the form of a cluster where the energy exchange between excitations is less effective than in a crystal. Through the point contact mode, it is ensured "the point contact" is on top of metallic substrate. We explore the sub-10-nm region where one can expect switching current reduction superior to that due to the linear scaling.

Figure 3D shows current versus resistance based on on/off states. In this regime, the thermal reservoir, which usually absorbs the energy of excitations, becomes extremely small and is unable to absorb the energy resulting from the magnetic dynamics. Further, the model of continuous crystalline lattice becomes invalid in this intermediate size range. A more suitable model would consider a material in the form of a cluster where the energy exchange between excitations is less effective than in a crystal in this range. The switching current is reduced by the small size of the contact region.

3. Conclusion

We investigated a new device that exploits the advantages of both the NEMS and spintronic technologies. Particularly, we demonstrated that nanomagnets placed on the NEM elements could be used as highly scalable non-volatile and robustly controlled memory. The STT switching experiments conducted on extremely high-anisotropy $L1_{(0)}$ phase media showed a remarkably energy-efficient switching capability. Given these advantages, this hybrid approach paves the way to the nanomechanical spin memory capable of ultra-high-density memory with ultra-fast data rates, more than adequate thermal stability for achieving a square bit as small as 2 nm on a side, given a pitch of 4 nm, corresponding to areal densities above 1 TB in^{-2}.

Acknowledgements

This work was supported by the National Natural Science Foundation of China under Award number 60674062, the U.S. Department of Energy, Office of Basic Energy Sciences, Division of Materials Sciences and Engineering under Contract No. DE-AC02-05CH11231.

Conflict of Interest

The authors declare no conflict of interest.

Data Availability Statement

The data that support the findings of this study are available from the corresponding author upon reasonable request.

Keywords

magnetic memory, MRAM, probe memory, probtronics, spintronics

Received: June 29, 2023
Published online:

[1] H. Ohno, M. D. Stiles, B. Dieny, *Proc IEEE Inst Electr Electron Eng* **2016**, *104*, 1782.

[2] J. S. Meena, S. M. Sze, U. Chand, T.-Y. Tseng, *Nano Res Lett* **2014**, *9*, 1.
[3] P. C. Lacaze, J.-C. Lacroix, *Non-volatile memories*, ISTE Ltd., London, UK **2014**.
[4] C. Zhao, C. Z. Zhao, S. Taylor, P. R. Chalker, *Materials* **2014**, *7*, 5117.
[5] G. W. Burr, M. J. Breitwisch, M. Franceschini, D. Garetto, K. Gopalakrishnan, B. Jackson, B. Kurdi, C. Lam, L. A. Lastras, A. Padilla, B. Rajendran, S. Raoux, R. S. Shenoy, *J Vac Sci Technol B* **2010**, *28*, 223.
[6] Q. Cao, W. Lü, X. R. Wang, X. Guan, L. Wang, S. Yan, T. Wu, X. Wang, *ACS Appl. Mater. Interfaces* **2020**, *12*, 42449.
[7] R. Waser, R. Dittmann, G. Staikov, K. Szot, *Adv. Mater.* **2009**, *21*, 2632.
[8] B. W. Soon, E. J. Ng, Y. Qian, N. Singh, M. J. Tsai, C. Lee, *Appl. Phys. Lett.* **2013**, *103*, 053122.
[9] C. J. Xue, *Handbook of Hardware/Software Codesign* (Eds: S. Ha, J. Teich), Springer, Dordrecht **2017**.
[10] Y. Kim, S. J. Kelly, A. Morozovska, E. K. Rahani, E. Strelcov, E. Eliseev, S. Jesse, M. D. Biegalski, N. Balke, N. Benedek, D. Strukov, J. Aarts, I. Hwang, S. Oh, J. S. Choi, T. Choi, B. H. Park, V. B. Shenoy, P. Maksymovych, S. V. Kalinin, *Nano Lett.* **2013**, *13*, 4068.
[11] J. Hong, M. Stone, B. Navarrete, K. Luongo, Q. Zheng, Z. Yuan, K. Xia, N. Xu, J. Bokor, L. You, S. Khizroev, *Appl. Phys. Lett.* **2018**, *112*, 112402.
[12] S. Ikeda, K. Miura, H. Yamamoto, K. Mizunuma, H. D. Gan, M. Endo, S. Kanai, J. Hayakawa, F. Matsukura, H. Ohno, *Nat. Mater.* **2010**, *9*, 721.